

SEMANTIC SELF-DISTILLATION FOR LANGUAGE MODEL UNCERTAINTY

Edward Phillips¹, Sean Wu¹, Boyan Gao¹, David A. Clifton^{1,2}

¹Department of Engineering Science, University of Oxford

²Oxford Suzhou Centre for Advanced Research

{edward.phillips, david.clifton}@eng.ox.ac.uk

ABSTRACT

Large language models present challenges for principled uncertainty quantification, in part due to their complexity and the diversity of their outputs. Semantic dispersion, or the variance in the meaning of sampled answers, has been proposed as a useful proxy for model uncertainty, but the associated computational cost prohibits its use in latency-critical applications. We show that sampled semantic distributions can be distilled into lightweight student models which estimate a prompt-conditioned uncertainty before the language model generates an answer token. The student model predicts a semantic distribution over possible answers; the entropy of this distribution provides an effective uncertainty signal for hallucination prediction, and the probability density allows candidate answers to be evaluated for reliability. On TriviaQA, our student models match or outperform finite-sample semantic dispersion for hallucination prediction and provide a strong signal for out-of-domain answer detection. We term this technique Semantic Self-Distillation (SSD), which we suggest provides a general framework for distilling predictive uncertainty in complex output spaces beyond language.

1 INTRODUCTION

Uncertainty quantification (UQ) can be used to assess the reliability of large language model (LLM) outputs (Xiong et al., 2024; Liu et al., 2025). As LLMs are rapidly deployed in high-stakes domains such as healthcare and law, it becomes increasingly important to have meaningful measures for the trustworthiness of model-generated content. Well-designed UQ methods can provide signals for detecting *hallucinations* - outputs that are misaligned with fact or user intention - and enable mitigation strategies such as abstention or optimal answer selection (Wen et al., 2025).

LLMs are now frequently embedded in *agentic frameworks*, which chain multiple model invocations to solve complex, multi-step challenges (Yao et al., 2023; Xi et al., 2025). In these settings a single unreliable output can result in an error which compounds destructively over long-horizon tasks, resulting in complete failure of the system to achieve its goal (Kwa et al., 2025). Given the computational burden of agentic frameworks, practical uncertainty estimators must be low latency compared to the base language models employed.

Semantic dispersion can be a useful proxy for uncertainty: when a language model generates multiple semantically distinct answers to the same prompt, the response is unlikely to be factual and correct. Measures based on semantic dispersion are effective for hallucination detection (Farquhar et al., 2024) but require generating many stochastic completions, rendering them prohibitively slow for latency-sensitive agentic applications.

Probing techniques can address this latency issue by employing lightweight models to predict semantic dispersion or hallucination probability directly from internal model representations (Kadavath et al., 2022; Obeso et al., 2025; Han et al., 2025; Kossen et al., 2024). However, these methods typically collapse the complex notion of language model uncertainty into a single scalar metric, ignoring the topology of the underlying output distribution. This lossy reduction limits their application to simple risk classification, preventing the extraction of richer reliability signals.

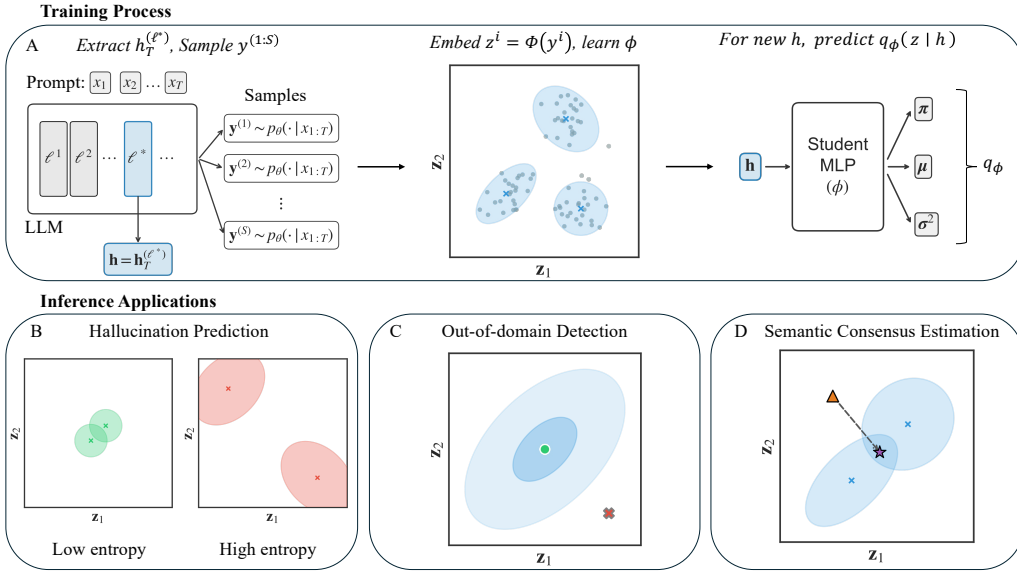


Figure 1: Overview of Semantic Self-Distillation (SSD). **(A) Training:** For each prompt, a hidden representation \mathbf{h} conditions a student that distils sampled answer embeddings into a semantic mixture distribution. **(B-D) Inference:** The predicted density supports pre-generation hallucination prediction via entropy, post-generation context verification via likelihood, and semantic consensus estimation via the mixture mean. Plots illustrate the semantic embedding space, where points denote sampled answers and the mixture mean represents the model’s semantic consensus.

In this work, we propose **Semantic Self-Distillation** (SSD), a general UQ framework which bridges simple probing techniques and expensive sampling-based methods. Instead of regressing a single scalar statistic, SSD trains a small student model to predict a prompt-conditioned distribution over semantic answer embeddings. We model the student as a mixture density network (MDN) (Bishop, 1994), and approximate the teacher distribution using stochastic samples from the base language model. The resulting density acts as a general-purpose uncertainty object: its analytic entropy provides a pre-generation risk forecast, while its posterior likelihood enables post-generation answer verification and other distribution-level operations. Figure 1 provides an overview of the SSD training procedure and the inference-time applications investigated in this work.

On the TriviaQA dataset, SSD provides hallucination-risk signals that in many cases improve upon finite-sample empirical dispersion estimates. Beyond hallucination classification, the distilled density supports (i) context verification via likelihood-based out-of-domain detection and (ii) semantic consensus estimation from a single forward pass.

We summarize our contributions as the following:

- We introduce **Semantic Self-Distillation**, a method for distilling a language model’s sampled semantic answer distribution into a lightweight conditional density estimator.
- We evaluate SSD for pre-generation hallucination prediction, characterizing its cost-accuracy trade-offs relative to sampling-based semantic dispersion and scalar probes.
- We demonstrate additional reliability primitives enabled by the predicted density, including post-generation verification via likelihood and single-pass semantic consensus estimation.

2 METHODS

2.1 PROBLEM SETUP

Let $x_{1:T}$ be an input prompt and $y_{1:L}$ a completion generated by an autoregressive model. Let $\mathbf{h} = f_\theta(x_{1:T}) \in \mathbb{R}^{d_h}$ denote a vector representation of the prompt extracted from the model’s

internal states. We define a semantic embedding $\mathbf{z} \in \mathbb{R}^{d_z}$ of the completed sequence via a mapping

$$\mathbf{z} = \Phi(y_{1:L}).$$

We train a student model $q_\phi(\mathbf{z} \mid \mathbf{h})$ to predict the distribution over semantic embeddings \mathbf{z} given only \mathbf{h} . The entropy of $q_\phi(\cdot \mid \mathbf{h})$ provides an uncertainty signal for hallucination prediction.

2.2 PROMPT AND ANSWER REPRESENTATIONS

Given a user prompt x of length T , we extract hidden states directly from the base language model. Let $\mathbf{h}_t^{(\ell)} \in \mathbb{R}^d$ denote the hidden state at layer ℓ for token position t . We utilize the representation of the *final token* of the prompt extracted from a single specific layer ℓ^* :

$$\mathbf{h} = \mathbf{h}_T^{(\ell^*)}.$$

The layer index ℓ^* is treated as a hyperparameter. In practice, we estimate the optimal ℓ^* by identifying the layer most predictive of the model’s semantic uncertainty, as detailed in Section 3.

For the answer, we apply a specialist embedding model to the generated sequence to obtain the semantic representation (see Section 3 for model details). To improve training efficiency and focus on the principal axes of semantic variation, we apply Principal Component Analysis (PCA) to the target embeddings \mathbf{z} . We fit the PCA transformation on the flattened set of stochastic training completions.

2.3 STUDENT DISTRIBUTION

We model the student as an MDN (Bishop, 1994). Conditioned on the prompt representation $\mathbf{h} \in \mathbb{R}^{d_h}$, the student predicts a K -component Gaussian mixture over the semantic embedding $\mathbf{z} \in \mathbb{R}^{d_z}$:

$$q_\phi(\mathbf{z} \mid \mathbf{h}) = \sum_{k=1}^K \pi_k(\mathbf{h}) \mathcal{N}(\mathbf{z}; \boldsymbol{\mu}_k(\mathbf{h}), \text{diag}(\boldsymbol{\sigma}_k^2(\mathbf{h}))),$$

$$\pi_k(\mathbf{h}) = \text{softmax}_k(\boldsymbol{\alpha}(\mathbf{h})),$$

where an MLP with parameters ϕ maps \mathbf{h} to mixture logits $\boldsymbol{\alpha}(\mathbf{h}) \in \mathbb{R}^K$, component means $\boldsymbol{\mu}_k(\mathbf{h}) \in \mathbb{R}^{d_z}$, and (log-)scales $\boldsymbol{\sigma}_k(\mathbf{h}) \in \mathbb{R}^{d_z}$. We train by maximizing the conditional log-likelihood of teacher samples. For data efficiency, we use diagonal covariances.

2.4 TEACHER CONSTRUCTION AND TRAINING

For each training prompt x , we extract the representation \mathbf{h} (using the selected layer ℓ^*) and generate S stochastic completions $y^{(1)}, \dots, y^{(S)}$. We compute semantic embeddings $\mathbf{z}^{(s)} = \Phi(y^{(s)})$ for $s=1, \dots, S$, and fit the student parameters ϕ by conditional maximum likelihood:

$$\max_{\phi} \sum_{\mathbf{x}} \frac{1}{S} \sum_{s=1}^S \log q_\phi(\mathbf{z}^{(s)} \mid \mathbf{h}).$$

2.5 QUANTIFYING DISPERSION

Given a new test prompt $x_{1:T}$, we compute its representation $\mathbf{h} = f_\theta(x_{1:T})$ in a single forward pass of the base model. The student then predicts the parameters of a K -component diagonal-covariance Gaussian mixture over semantic embeddings. We measure dispersion using the order-2 Rényi entropy (Rényi, 1961) of the predictive density:

$$H_2(q_\phi(\cdot \mid \mathbf{h})) = -\log \int q_\phi(\mathbf{z} \mid \mathbf{h})^2 d\mathbf{z},$$

Intuitively, the integral $\int q(\mathbf{z})^2 d\mathbf{z}$ is the *collision probability* of the density: it is larger when mass is concentrated, and smaller when the distribution is spread out (Principe, 2010). Higher H_2 corresponds to greater semantic dispersion.

We use Rényi-2 because it yields an exact closed form for Gaussian mixtures (Wang et al., 2009), enabling a sampling-free, analytic dispersion score at inference time. By contrast, the Shannon differential entropy (Shannon, 1948) does not, in general, admit a closed-form expression for Gaussian mixture models; it is typically approximated using Monte Carlo estimation or via analytic bounds (Huber et al., 2008; Dahlke & Pacheco, 2023). Using Rényi-2 therefore preserves SSD’s goal of avoiding additional sampling or expensive numerical estimation at deployment. We provide the closed form expression and derivation in Appendix Section A.

2.6 USING THE PREDICTED SEMANTIC DISTRIBUTION

At inference time, SSD produces a prompt-conditioned semantic density $q_\phi(\mathbf{z} \mid \mathbf{h})$ over answer embeddings, which we treat as a general-purpose uncertainty object with three primitive operations:

(i) Semantic Dispersion Prediction We use the Rényi-2 entropy $H_2(q_\phi(\cdot \mid \mathbf{h}))$ to provide a prompt-level uncertainty estimate in a single forward pass.

(ii) Context Verification Given any candidate response \mathbf{y}' , we embed it as $\mathbf{z}' = \Phi(\mathbf{y}')$ and score its compatibility with the prompt via the posterior log-likelihood $\log q_\phi(\mathbf{z}' \mid \mathbf{h})$. We treat answers with low likelihood as out-of-domain relative to the prompt context.

(iii) Latent Sampling Because $q_\phi(\mathbf{z} \mid \mathbf{h})$ is an explicit mixture distribution, we can compute summary statistics such as the mixture mean $\mathbb{E}_{q_\phi}[\mathbf{z}] = \sum_k \pi_k(\mathbf{h}) \boldsymbol{\mu}_k(\mathbf{h})$ and, when desired, draw latent samples $\tilde{\mathbf{z}} \sim q_\phi(\cdot \mid \mathbf{h})$.

3 EXPERIMENTS

3.1 MODELS AND DATASET GENERATION

We evaluate the SSD distribution in the context of short-form question answering, using the TriviaQA dataset (Joshi et al., 2017). We construct a training set of $N_{train} = 4000$ prompts and report results on a held-out test set of $N_{test} = 1000$ prompts.

We evaluate across five model families: **Mistral** (Minstral-8B-Instruct), **Llama-3** (3.1-8B-Instruct, 3.2-3B-Instruct), **Qwen** (Qwen3-4B-Instruct-2507, Qwen3-8B), **Gemma** (Gemma-3-4B) and **SmollM** (SmollM3-3B). For all experiments, we use Qwen3-8B as the oracle ‘judge’ model to determine the correctness of generated answers.

For each prompt and model, we sample $S = 32$ samples at temperature $T = 1$. We additionally sample a single ‘default’ answer at $T = 0.1$ which we input to the judge model to generate the hallucination label.

For the answer embedding, we use EmbeddingGemma (Vera et al., 2025), with the embedding truncated to a dimension of $d_z = 128$. For hallucination detection, we further reduce dimensionality using PCA to $d'_z = 16$, following ablation studies detailed in Appendix Section D. For likelihood-based OOD verification, we set $d'_z = 32$.

3.2 LAYER SELECTION PROTOCOL

To estimate a suitable layer ℓ^* for the student input, we use the results of our hallucination detection baseline experiments, described in Section 3.3. Following Kossen et al. (2024), we first train simple linear probes on all layers to predict the binarized Semantic Entropy. We select the layer index ℓ^* that maximizes validation accuracy for this proxy task. We assume that the layer most predictive of the scalar entropy value also contains the richest information for constructing the full distributional mixture. We find this typically corresponds to deeper layers, shown in Table 5 in the Appendix.

Model	AUROC		AUPRC	
	TD	SSD	TD	SSD
Qwen3-8B	0.684 ± 0.017	0.677 ± 0.018	0.525 ± 0.027	0.570 ± 0.028
Qwen3-4B	0.732 ± 0.016	0.699 ± 0.016	0.596 ± 0.025	0.618 ± 0.025
Llama 3.1 8B	0.695 ± 0.017	0.686 ± 0.020	0.443 ± 0.028	0.519 ± 0.030
Llama 3.2 3B	0.665 ± 0.017	0.738 ± 0.017	0.558 ± 0.027	0.657 ± 0.027
Minstral 8B	0.743 ± 0.016	0.748 ± 0.016	0.579 ± 0.029	0.599 ± 0.029
SmollM3 3B	0.698 ± 0.016	0.711 ± 0.016	0.569 ± 0.025	0.623 ± 0.026
Gemma 3 4B	0.676 ± 0.017	0.701 ± 0.017	0.632 ± 0.024	0.662 ± 0.025

Table 1: **Distilling sampled dispersion into a single pass.** TD computes dispersion from $S = 32$ sampled semantic embeddings at inference time, while SSD predicts a prompt-conditioned semantic density and scores dispersion analytically. We report hallucination detection AUROC/AUPRC as mean \pm standard deviation over 1,000 bootstrap resamples of the test set; bold indicates the better of TD vs. SSD per metric.

3.3 HALLUCINATION DETECTION VIA PREDICTED DISPERSION

We treat the student’s dispersion score as a *pre-generation* risk score: higher values indicate greater semantic spread and higher hallucination risk. We report AUROC and AUPRC against correctness labels determined using an LLM-as-judge framework.

SSD compares favourably to teacher dispersion. We first compare the student’s dispersion score to the standard deviation of the teacher’s $S = 32$ semantic embeddings, which we term *teacher dispersion* (TD). Table 1 reports results across models. Despite requiring no inference-time sampling, SSD outperforms TD on four of the seven models investigated in AUROC and on all seven in AUPRC. We attribute this in part to a smoothing effect: TD is a finite-sample statistic and assigns zero uncertainty to prompts where the model consistently produces the same answer, even when that answer is incorrect. By contrast, SSD learns a continuous mapping from prompt representations to semantic uncertainty, enabling differentiated risk estimates in such degenerate cases, which likely contributes to its stronger AUPRC.

Comparison to additional baselines. We further compare SSD against three widely used hallucination detection methods:

1. **Probability of Correctness Probe (PCP):** A logistic regression classifier trained on the prompt representation to predict binary correctness. Originally proposed as ‘P(I know)’ by Kadavath et al. (2022), this method requires externally provided correctness labels.
2. **Semantic Entropy (SE):** A state-of-the-art sampling-based approach that measures semantic dispersion by clustering S stochastic completions using a natural language inference (NLI) model to assess mutual entailment (Farquhar et al., 2024).
3. **Semantic Entropy Probe (SEP):** A lightweight probe with the same architecture as PCP, trained to regress a binarized SE target, inheriting SE’s sampling and NLI-based target construction cost (Kossen et al., 2024).

To reflect agentic deployment constraints, we report hallucination detection performance alongside method characteristics: inference latency, supervision target construction cost, and whether a method supports post-generation (posterior) signals in addition to pre-generation (prior) uncertainty. Table 2 summarizes these trade-offs and reports macro-average AUROC across model families; full per-model AUROC/AUPRC tables are provided in the Appendix (tables 8 and 9).

Overall, SE achieves the strongest AUROC, consistent with prior work showing that explicit sampling of multiple reasoning paths yields high-quality uncertainty signals (Kadavath et al., 2022). Among single-pass methods, PCP and SEP outperform SSD as pre-generation hallucination predictors, confirming that the binary classification problem is simpler than distilling the geometry of a full semantic distribution. However, SSD occupies a distinct and practically useful regime: it matches

Method	AUROC \uparrow	Latency \downarrow	Target cost \downarrow	Posterior
SE	0.804 \pm 0.036	S samples + S^2 NLI	–	✗
SEP	0.759 \pm 0.026	Single-pass	S samples + S^2 NLI	✗
PCP	0.771 \pm 0.021	Single-pass	C_{CL}	✗
TD	0.699 \pm 0.027	S samples	–	✗
SSD	0.708 \pm 0.024	Single-pass	S samples + S Φ	$\ell(y), \mathbb{E}[\mathbf{z}]$

Table 2: **Hallucination detection trade-offs.** AUROC is reported as a macro-average (mean \pm std) across models. Latency summarizes inference-time requirements (single-pass vs S sampled generations, with entailment-based SE additionally requiring S^2 natural language inference (NLI) comparisons). Target cost denotes the computation required to construct supervision targets during training; C_{CL} is the cost of acquiring correctness labels. Only SSD explicitly provides post-generation posterior signals in addition to pre-generation uncertainty.

probe-level inference latency, avoids entailment-based target construction, and uniquely provides posterior signals as well as prior risk scores. The post-generation signals enable verification and filtering mechanisms that are not available to scalar probes.

3.4 DISTILLATION FIDELITY VS. DETECTION PERFORMANCE

We examine whether the quality of distillation (how closely the student learns the teacher distribution) constrains hallucination detection performance. We define *distillation fidelity* (ρ_{fidelity}) as the Spearman rank correlation, over $N = 1000$ test prompts, between the student’s predicted entropy and the teacher dispersion. A high ρ_{fidelity} indicates a more faithful recovery of the teacher’s prompt-induced uncertainty ordering.

Figure 2 plots hallucination detection AUROC against distillation fidelity across base models and student hyperparameter settings. We observe a strong positive relationship, with a cross-model Spearman correlation of $\rho_{\text{meta}} = 0.65$, indicating that detection performance is limited by the student’s ability to learn the prompt-to-dispersion mapping. The failure cases, notably Qwen3-4B, exhibit near-zero ρ_{fidelity} , suggesting that the relevant uncertainty signal is not accessible from the chosen prompt representation.

3.5 CONTEXT VERIFICATION VIA OUT-OF-DOMAIN DETECTION

We evaluate the SSD density as a post-generation verification signal by measuring its ability to detect mismatched prompt-answer pairs. We frame this as an out-of-domain detection task: for each test prompt x_i , we pair its representation \mathbf{h}_i with (i) the model’s default answer y_i and (ii) a random answer y_j drawn from a different prompt. Each candidate answer is embedded as $\mathbf{z} = \Phi(y)$ and scored using the student’s posterior log-likelihood $\log q_\phi(\mathbf{z} \mid \mathbf{h})$. We report AUROC for distinguishing matched from mismatched pairs.

As shown in Table 3, the posterior likelihood is a strong context-verification signal, achieving AUROCs above 0.95 for most base models. This suggests that SSD can serve as a low-latency guardrail in agentic workflows, for example detecting cache poisoning (Chen et al., 2024) or filtering retrieved content in retrieval-augmented generation (Lewis et al., 2020).

The likelihood provides a modest signal for *post-generation* hallucination detection, demonstrated by AUROCs above 0.5. This result could be interpreted through the lens of Semantic Density (Qiu & Miikkulainen, 2024), which posits that reliable samples tend to lie in denser regions of a semantic predictive space. Rather than approximating this distribution via samples and associated sequence likelihoods, our approach explicitly models it.

3.6 SEMANTIC CONSENSUS FROM THE PREDICTED MIXTURE

We evaluate the generative utility of the student by measuring its ability to approximate the semantic consensus of the model. We treat the empirical mean of $S = 32$ stochastic samples as a reference semantic centroid, then measure the mean squared distance (MSD) in Euclidean space between

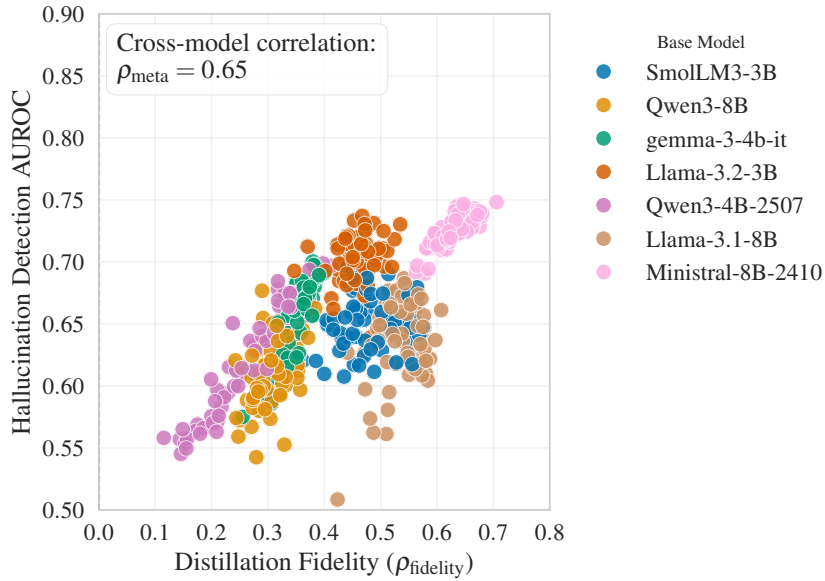


Figure 2: **Distillation fidelity drives detection performance.** The X-axis shows *distillation fidelity* (ρ_{fidelity}): the Spearman correlation between the student’s predicted entropy and the teacher dispersion across test prompts. Multiple points per model correspond to different student hyperparameter settings. ρ_{meta} is the Spearman correlation between the X and Y variables; it shows that models where the student fails to learn the distribution (low ρ_{fidelity}) result in poor detection.

Table 3: **Utility of SSD posterior likelihood.** Out-of-domain (OOD) detection reports AUROC for distinguishing an answer belonging to the prompt from a random answer. Hallucination detection compares AUROC for pre-generation entropy vs. post-generation likelihood. While likelihood is a strong OOD detector, entropy remains the superior signal for hallucination classification. Values report mean AUROC with bootstrap standard deviation over 1,000 resamples.

Model	OOD		Hallucination	
	Likelihood	Entropy	Likelihood	Entropy
Qwen3 8B	0.983 ± 0.002	0.697 ± 0.017	0.571 ± 0.019	
Qwen3 4B	0.984 ± 0.002	0.703 ± 0.016	0.555 ± 0.018	
Llama 3.1 8B	0.989 ± 0.002	0.702 ± 0.019	0.578 ± 0.020	
Llama 3.2 3B	0.980 ± 0.003	0.728 ± 0.016	0.612 ± 0.018	
Minstral 8B	0.944 ± 0.005	0.758 ± 0.016	0.616 ± 0.018	
SmolLM3 3B	0.988 ± 0.002	0.676 ± 0.018	0.563 ± 0.018	
Gemma 3 4B	0.895 ± 0.007	0.679 ± 0.017	0.577 ± 0.018	

this centroid and both (i) the model’s low-temperature output and (ii) the analytical mean of the student mixture, $\mu_{\text{ssd}} = \sum_k \pi_k \mu_k$. Lower MSD indicates better recovery of the model’s aggregate semantic belief. MSD is computed as $\mathbb{E}_i [\|\hat{\mathbf{z}}_i - \mu_i^{\text{true}}\|_2^2]$ over examples i in the subset.

We report results for the best-performing student configuration (Minstral 8B), reflecting the strong architectural dependence of distillation fidelity. As shown in Table 4, the SSD mixture mean provides a closer approximation to the semantic centroid than a single default decoding pass. This effect is most pronounced for incorrect answers, where SSD improves centroid recovery in over 76% of test cases. This aligns with prior work showing that hallucinated outputs tend to deviate from semantic consensus (Lin et al., 2024; Phillips et al., 2025). Together with the OOD results in Table 3, this result suggests that SSD’s pre-generation uncertainty estimates can be complemented by post-generation distance- and likelihood-based checks derived from the same predicted density.

Table 4: Semantic consensus approximation with Minstral 8B. We report the mean squared distance (MSD) of the default answer embedding and the SSD predicted mean to the true semantic centroid (average of $S = 32$ samples). Values denote mean MSD, with the bootstrap standard deviation expressed as a percentage of the mean shown as a subscript.

Subset	Default MSD ↓	SSD MSD ↓	Imp. (%) ↑	SSD Win Rate (%) ↑
All	0.015 _{3.2}	0.008_{1.9}	+45.5	58.3
Correct	0.013 _{4.4}	0.009_{2.3}	+32.3	48.8
Incorrect	0.018 _{4.2}	0.007_{3.4}	+63.0	76.5

4 FUTURE WORK

Improving distillation fidelity. Our results indicate that SSD’s utility as a pre-generation hallucination signal is primarily limited by distillation fidelity: detection performance improves when the student accurately recovers the teacher’s prompt-induced uncertainty ordering. Promising directions include scaling the distillation dataset, enriching the student input beyond a single-token/single-layer representation, and distilling from stronger teachers (larger S , or higher-quality semantic targets). These extensions would clarify whether observed failures reflect an information bottleneck in the prompt representation or insufficient supervision for density estimation.

Combining prior and posterior signals. SSD exposes complementary reliability signals from a single predicted density: pre-generation dispersion forecasts risk, while post-generation likelihood and distance-to-consensus verify prompt–answer agreement. A natural next step is to integrate these signals into decision policies for agents, for example abstaining or retrieving evidence under high dispersion, and accepting or rejecting candidate actions based on likelihood or consensus distance.

Diffusion models. While we focus on autoregressive models, SSD may be particularly well suited to diffusion-based language models, where hidden prompt representations may more directly parameterize the final semantic output distribution (Sahoo et al., 2024).

Domain-specific uncertainty estimation. The technique naturally extends to domain-specific foundation models, such as those in healthcare (Renc et al., 2024; Steinberg et al., 2024) and time-series forecasting (Faw et al., 2025). By distilling predictive distributions over latent outcome representations, students could provide real-time uncertainty estimates for future patient trajectories or other temporal processes, enabling risk-aware decision-making in sequential settings (Zeng et al., 2025).

5 CONCLUSION

We introduced Semantic Self-Distillation (SSD), a distributional probing framework that distils a language model’s sampled semantic answer distribution into a lightweight, prompt-conditioned density estimator. Unlike scalar probes which compress uncertainty into a single score, SSD predicts an explicit semantic density, enabling analytic dispersion scoring and additional distribution-level operations in a single forward pass.

Empirically, SSD provides competitive hallucination-risk signals relative to finite-sample baselines on several model families, while avoiding the inference-time overhead of generating multiple completions. Crucially, modelling the full density unlocks capabilities that scalar probes cannot match: the posterior likelihood provides strong context verification checks for out-of-domain answers, while mixture statistics allow for single-pass semantic consensus estimates.

Overall, SSD demonstrates that distilling a semantic predictive distribution can yield a general-purpose uncertainty object with applications in forecasting and verification. By decoupling these capabilities from expensive inference-time sampling, SSD offers a practical framework for integrating principled uncertainty quantification into latency-critical agentic applications.

6 ACKNOWLEDGMENTS

DAC was funded by an NIHR Research Professorship; a Royal Academy of Engineering Research Chair; and the InnoHK Hong Kong Centre for Cerebro-cardiovascular Engineering (COCHE); and was supported by the National Institute for Health Research (NIHR) Oxford Biomedical Research Centre (BRC) and the Pandemic Sciences Institute at the University of Oxford. EP was funded by an NIHR Research Studentship. SW was supported by the Rhodes Scholarship.

REFERENCES

Christopher M. Bishop. Mixture density networks. Copyright © 1994, Christopher M. Bishop. This work is licensed under a Creative Commons Attribution-NonCommercial-NoDerivatives 4.0 International License (<https://creativecommons.org/licenses/by-nc-nd/4.0/>), 1994. URL <https://publications aston.ac.uk/id/eprint/373/>. 2, 3

Zhaorun Chen, Zhen Xiang, Chaowei Xiao, Dawn Song, and Bo Li. Agentpoison: Red-teaming llm agents via poisoning memory or knowledge bases. In A. Globerson, L. Mackey, D. Belgrave, A. Fan, U. Paquet, J. Tomczak, and C. Zhang (eds.), *Advances in Neural Information Processing Systems*, volume 37, pp. 130185–130213. Curran Associates, Inc., 2024. doi: 10.52202/079017-4136. URL https://proceedings.neurips.cc/paper_files/paper/2024/file/eb113910e9c3f6242541c1652e30dfd6-Paper-Conference.pdf. 6

Caleb Dahlke and Jason Pacheco. On convergence of polynomial approximations to the gaussian mixture entropy. In A. Oh, T. Naumann, A. Globerson, K. Saenko, M. Hardt, and S. Levine (eds.), *Advances in Neural Information Processing Systems*, volume 36, pp. 75469–75490. Curran Associates, Inc., 2023. URL https://proceedings.neurips.cc/paper_files/paper/2023/file/ee860a9fa65a55a335754c557a5211de-Paper-Conference.pdf. 4

Sebastian Farquhar, Jannik Kossen, Lorenz Kuhn, and Yarin Gal. Detecting hallucinations in large language models using semantic entropy. *Nature*, 630(8017):625–630, June 2024. ISSN 1476-4687. doi: 10.1038/s41586-024-07421-0. URL <https://www.nature.com/articles/s41586-024-07421-0>. Publisher: Nature Publishing Group. 1, 5, 13

Matthew Faw, Rajat Sen, Yichen Zhou, and Abhimanyu Das. In-context fine-tuning for time-series foundation models. In *Forty-second International Conference on Machine Learning*, 2025. URL <https://openreview.net/forum?id=uxzgGLWPj2>. 8

Jiatong Han, Neil Band, Muhammed Razzak, Jannik Kossen, Tim G. J. Rudner, and Yarin Gal. Simple factuality probes detect hallucinations in long-form natural language generation. In Christos Christodoulopoulos, Tanmoy Chakraborty, Carolyn Rose, and Violet Peng (eds.), *Findings of the Association for Computational Linguistics: EMNLP 2025*, pp. 16209–16226, Suzhou, China, November 2025. Association for Computational Linguistics. ISBN 979-8-89176-335-7. doi: 10.18653/v1/2025.findings-emnlp.880. URL <https://aclanthology.org/2025.findings-emnlp.880>. 1

Marco F Huber, Tim Bailey, Hugh Durrant-Whyte, and Uwe D Hanebeck. On entropy approximation for gaussian mixture random vectors. In *2008 IEEE International Conference on Multisensor Fusion and Integration for Intelligent Systems*, pp. 181–188. IEEE, 2008. 4

Mandar Joshi, Eunsol Choi, Daniel Weld, and Luke Zettlemoyer. TriviaQA: A large scale distantly supervised challenge dataset for reading comprehension. In Regina Barzilay and Min-Yen Kan (eds.), *Proceedings of the 55th Annual Meeting of the Association for Computational Linguistics (Volume 1: Long Papers)*, pp. 1601–1611, Vancouver, Canada, July 2017. Association for Computational Linguistics. doi: 10.18653/v1/P17-1147. URL <https://aclanthology.org/P17-1147>. 4

Saurav Kadavath, Tom Conerly, Amanda Askell, Tom Henighan, Dawn Drain, Ethan Perez, Nicholas Schiefer, Zac Hatfield-Dodds, Nova DasSarma, Eli Tran-Johnson, Scott Johnston, Sheer El-Showk, Andy Jones, Nelson Elhage, Tristan Hume, Anna Chen, Yuntao Bai, Sam Bowman, Stanislav Fort, Deep Ganguli, Danny Hernandez, Josh Jacobson, Jackson Kernion, Shauna Kravec, Liane Lovitt, Kamal Ndousse, Catherine Olsson, Sam Ringer, Dario Amodei, Tom Brown, Jack Clark, Nicholas Joseph, Ben Mann, Sam McCandlish, Chris Olah, and Jared Kaplan. Language models (mostly) know what they know, 2022. URL <https://arxiv.org/abs/2207.05221>. 1, 5

Jannik Kossen, Jiatong Han, Muhammed Razzak, Lisa Schut, Shreshth Malik, and Yarin Gal. Semantic entropy probes: Robust and cheap hallucination detection in llms, 2024. URL <https://arxiv.org/abs/2406.15927>. 1, 4, 5

Thomas Kwa, Ben West, Joel Becker, Amy Deng, Katharyn Garcia, Max Hasin, Sami Jawhar, Megan Kinniment, Nate Rush, Sydney Von Arx, Ryan Bloom, Thomas Broadley, Haoxing Du, Brian Goodrich, Nikola Jurkovic, Luke Harold Miles, Seraphina Nix, Tao Roa Lin, Neev Parikh, David Rein, Lucas Jun Koba Sato, Hjalmar Wijk, Daniel M Ziegler, Elizabeth Barnes, and Lawrence Chan. Measuring AI ability to complete long software tasks. In *The Thirty-ninth Annual Conference on Neural Information Processing Systems*, 2025. URL <https://openreview.net/forum?id=CGNJL6CeV0.1>

Patrick Lewis, Ethan Perez, Aleksandra Piktus, Fabio Petroni, Vladimir Karpukhin, Naman Goyal, Heinrich Kütter, Mike Lewis, Wen-tau Yih, Tim Rocktäschel, Sebastian Riedel, and Douwe Kiela. Retrieval-augmented generation for knowledge-intensive nlp tasks. In H. Larochelle, M. Ranzato, R. Hadsell, M.F. Balcan, and H. Lin (eds.), *Advances in Neural Information Processing Systems*, volume 33, pp. 9459–9474. Curran Associates, Inc., 2020. URL https://proceedings.neurips.cc/paper_files/paper/2020/file/6b493230205f780e1bc26945df7481e5-Paper.pdf. 6

Zhen Lin, Shubhendu Trivedi, and Jimeng Sun. Generating with confidence: Uncertainty quantification for black-box large language models. *Transactions on Machine Learning Research*, 2024. ISSN 2835-8856. URL <https://openreview.net/forum?id=DWkJCSxKU5.7>

Xiaou Liu, Tiejin Chen, Longchao Da, Chacha Chen, Zhen Lin, and Hua Wei. Uncertainty quantification and confidence calibration in large language models: A survey. In *Proceedings of the 31st ACM SIGKDD Conference on Knowledge Discovery and Data Mining* V.2, KDD '25, pp. 6107–6117, New York, NY, USA, 2025. Association for Computing Machinery. ISBN 9798400714542. doi: 10.1145/3711896.3736569. URL <https://doi.org/10.1145/3711896.3736569.1>

Oscar Obeso, Andy Ardit, Javier Ferrando, Joshua Freeman, Cameron Holmes, and Neel Nanda. Real-time detection of hallucinated entities in long-form generation, 2025. URL <https://arxiv.org/abs/2509.03531.1>

Edward Phillips, Sean Wu, Soheila Molaei, Danielle Belgrave, Anshul Thakur, and David Clifton. Geometric uncertainty for detecting and correcting hallucinations in llms, 2025. URL <https://arxiv.org/abs/2509.13813.7>

Jose C Principe. *Information theoretic learning: Renyi's entropy and kernel perspectives*. Springer Science & Business Media, 2010. 3

Xin Qiu and Risto Miikkulainen. Semantic density: Uncertainty quantification for large language models through confidence measurement in semantic space. In A. Globerson, L. Mackey, D. Belgrave, A. Fan, U. Paquet, J. Tomczak, and C. Zhang (eds.), *Advances in Neural Information Processing Systems*, volume 37, pp. 134507–134533. Curran Associates, Inc., 2024. doi: 10.52202/079017-4274. URL https://proceedings.neurips.cc/paper_files/paper/2024/file/f26d4fbaf7dfa115f1d4b3f104e26bce-Paper-Conference.pdf.6

Pawel Renc, Yugang Jia, Anthony E Samir, Jaroslaw Was, Quanzheng Li, David W Bates, and Arkadiusz Sitek. Zero shot health trajectory prediction using transformer. *NPJ digital medicine*, 7(1):256, 2024. 8

Alfréd Rényi. On measures of entropy and information. In *Proceedings of the fourth Berkeley symposium on mathematical statistics and probability, volume 1: contributions to the theory of statistics*, volume 4, pp. 547–562. University of California Press, 1961. 3

Subham Sekhar Sahoo, Marianne Arriola, Yair Schiff, Aaron Gokaslan, Edgar Marroquin, Justin T Chiu, Alexander Rush, and Volodymyr Kuleshov. Simple and effective masked diffusion language models. In A. Globerson, L. Mackey, D. Belgrave, A. Fan, U. Paquet, J. Tomczak, and C. Zhang (eds.), *Advances in Neural Information Processing Systems*, volume 37, pp. 130136–130184. Curran Associates, Inc., 2024. doi: 10.52202/079017-4135. URL https://proceedings.neurips.cc/paper_files/paper/2024/file/eb0b13cc515724ab8015bc978fdde0ad-Paper-Conference.pdf.8

Claude E Shannon. A mathematical theory of communication. *The Bell system technical journal*, 27(3):379–423, 1948. 4

Ethan Steinberg, Jason Alan Fries, Yizhe Xu, and Nigam Shah. MOTOR: A time-to-event foundation model for structured medical records. In *The Twelfth International Conference on Learning Representations*, 2024. URL <https://openreview.net/forum?id=Nialiwi2V6>. 8

Henrique Schechter Vera, Sahil Dua, Biao Zhang, Daniel Salz, Ryan Mullins, Sindhu Raghuram Panyam, Sara Smoot, Iftekhar Naim, Joe Zou, Feiyang Chen, Daniel Cer, Alice Lisak, Min Choi, Lucas Gonzalez, Omar Sanseviero, Glenn Cameron, Ian Ballantyne, Kat Black, Kaifeng Chen, Weiyi Wang, Zhe Li, Gus Martins, Jinhyuk Lee, Mark Sherwood, Juyeong Ji, Renjie Wu, Jingxiao Zheng, Jyotinder Singh, Abheesht Sharma, Divyashree Sreepathihalli, Aashi Jain, Adham Elarabawy, AJ Co, Andreas Doumanoglou, Babak Samari, Ben Hora, Brian Potetz, Dahun Kim, Enrique Alfonseca, Fedor Moiseev, Feng Han, Frank Palma Gomez, Gustavo Hernández Ábrego, Hesen Zhang, Hui Hui, Jay Han, Karan Gill, Ke Chen, Koert Chen, Madhuri Shanbhogue, Michael Boratko, Paul Suganthan, Sai Meher Karthik Duddu, Sandeep Mariserla, Setareh Ariaifar, Shanfeng Zhang, Shijie Zhang, Simon Baumgartner, Sonam Goenka, Steve Qiu, Tanmaya Dabral, Trevor Walker, Vikram Rao, Waleed Khawaja, Wenlei Zhou, Xiaoqi Ren, Ye Xia, Yichang Chen, Yi-Ting Chen, Zhe Dong, Zhongli Ding, Francesco Visin, Gaël Liu, Jiageng Zhang, Kathleen Keanealy, Michelle Casbon, Ravin Kumar, Thomas Mesnard, Zach Gleicher, Cormac Brick, Olivier Lacombe, Adam Roberts, Qin Yin, Yunhsuan Sung, Raphael Hoffmann, Tris Warkentin, Armand Joulin, Tom Duerig, and Mojtaba Seyedhosseini. Embeddinggemma: Powerful and lightweight text representations, 2025. URL <https://arxiv.org/abs/2509.20354>. 4

Fei Wang, Tanveer Syeda-Mahmood, Baba C Vemuri, David Beymer, and Anand Rangarajan. Closed-form jensen-renyi divergence for mixture of gaussians and applications to group-wise shape registration. In *International Conference on Medical Image Computing and Computer-Assisted Intervention*, pp. 648–655. Springer, 2009. 4

Bingbing Wen, Jihan Yao, Shangbin Feng, Chenjun Xu, Yulia Tsvetkov, Bill Howe, and Lucy Lu Wang. Know your limits: A survey of abstention in large language models. *Transactions of the Association for Computational Linguistics*, 13:529–556, 2025. doi: 10.1162/tacl_a_00754. URL <https://aclanthology.org/2025.tacl-1.26/>. 1

Zhiheng Xi, Wenxiang Chen, Xin Guo, Wei He, Yiwen Ding, Boyang Hong, Ming Zhang, Junzhe Wang, Senjie Jin, Enyu Zhou, et al. The rise and potential of large language model based agents: A survey. *Science China Information Sciences*, 68(2):121101, 2025. 1

Miao Xiong, Andrea Santilli, Michael Kirchhof, Adam Golinski, and Sinead Williamson. Efficient and effective uncertainty quantification for LLMs. In *Neurips Safe Generative AI Workshop 2024*, 2024. URL <https://openreview.net/forum?id=QKRLH57ATT>. 1

Shunyu Yao, Jeffrey Zhao, Dian Yu, Nan Du, Izhak Shafran, Karthik R Narasimhan, and Yuan Cao. React: Synergizing reasoning and acting in language models. In *The Eleventh International Conference on Learning Representations*, 2023. URL https://openreview.net/forum?id=WE_vluYUL-X. 1

Sihang Zeng, Lucas Jing Liu, Jun Wen, Meliha Yetisgen, Ruth Etzioni, and Gang Luo. Trajsurv: Learning continuous latent trajectories from electronic health records for trustworthy survival prediction, 2025. URL <https://arxiv.org/abs/2508.00657>. 8

A DERIVATIONS

Closed-form computation of Rényi-2 entropy. For a Gaussian mixture, the quadratic functional $\int q(\mathbf{z})^2 d\mathbf{z}$ decomposes into pairwise overlaps between mixture components:

$$\int q_\phi(\mathbf{z} \mid \mathbf{h})^2 d\mathbf{z} = \sum_{i=1}^K \sum_{j=1}^K \pi_i(\mathbf{h}) \pi_j(\mathbf{h}) \int \mathcal{N}(\mathbf{z}; \boldsymbol{\mu}_i, \boldsymbol{\Sigma}_i) \mathcal{N}(\mathbf{z}; \boldsymbol{\mu}_j, \boldsymbol{\Sigma}_j) d\mathbf{z}.$$

Using the standard Gaussian product identity,

$$\int \mathcal{N}(\mathbf{z}; \boldsymbol{\mu}_i, \boldsymbol{\Sigma}_i) \mathcal{N}(\mathbf{z}; \boldsymbol{\mu}_j, \boldsymbol{\Sigma}_j) d\mathbf{z} = \mathcal{N}(\boldsymbol{\mu}_i; \boldsymbol{\mu}_j, \boldsymbol{\Sigma}_i + \boldsymbol{\Sigma}_j),$$

we obtain:

$$H_2(q_\phi(\cdot \mid \mathbf{h})) = -\log \left(\sum_{i=1}^K \sum_{j=1}^K \pi_i(\mathbf{h}) \pi_j(\mathbf{h}) \mathcal{N}(\boldsymbol{\mu}_i(\mathbf{h}); \boldsymbol{\mu}_j(\mathbf{h}), \boldsymbol{\Sigma}_i(\mathbf{h}) + \boldsymbol{\Sigma}_j(\mathbf{h})) \right).$$

Equivalently, defining the collision matrix $\mathbf{K}(\mathbf{h}) \in \mathbb{R}^{K \times K}$ with entries

$$K_{ij}(\mathbf{h}) = \mathcal{N}(\boldsymbol{\mu}_i(\mathbf{h}); \boldsymbol{\mu}_j(\mathbf{h}), \boldsymbol{\Sigma}_i(\mathbf{h}) + \boldsymbol{\Sigma}_j(\mathbf{h})),$$

and $\boldsymbol{\pi}(\mathbf{h}) \in \mathbb{R}^K$ the mixture weights, we have

$$H_2(q_\phi(\cdot \mid \mathbf{h})) = -\log(\boldsymbol{\pi}(\mathbf{h})^\top \mathbf{K}(\mathbf{h}) \boldsymbol{\pi}(\mathbf{h})).$$

This computation is $\mathcal{O}(K^2)$ in the number of mixture components and is negligible relative to the transformer backbone.

B MODEL METADATA

Table 5: Model characteristics. ‘Base Acc’ denotes QA accuracy. ‘PCP’ and ‘SEP’ indicate optimal probe layers. The ‘Best SSD Config’ columns show the student architecture (H =Hidden, D =Depth, K =Components) that achieved the highest SSD AUROC.

Model	Base Acc	Probe Layers		Best SSD Config			AUROC
		PCP	SEP	H	D	K	
Qwen3-8B	0.620	32	24	128	6	10	0.677
Qwen3-4B-Instruct-2507	0.565	18	20	256	2	10	0.699
Llama 3.1 8B	0.700	20	16	256	4	2	0.687
Llama 3.2 3B	0.585	15	19	512	3	5	0.737
Minstral 8B	0.656	33	34	1024	6	1	0.748
SmolLM3 3B	0.567	20	19	512	6	5	0.710
Gemma 3 4B	0.532	22	19	512	2	10	0.700

C COMPUTATIONAL COMPLEXITY ANALYSIS

The primary motivation for Semantic Self-Distillation is to enable generic uncertainty estimation in AR models without sampling. Here we compare the asymptotic complexity of our method against sampling-based baselines. Let T_{pre} be the prompt length, T_{gen} be the generation length, S be the number of samples, and C_{LLM} be the cost of a single transformer forward pass per token.

Sampling-based Methods (SE, TD). Computing Semantic Entropy (Farquhar et al., 2024) requires S stochastic sequences per prompt at inference time (typically $S \in [5, 20]$). The cost is dominated by the autoregressive decoding steps:

$$\mathcal{O}_{\text{SE}} \approx S \times (T_{\text{pre}} + T_{\text{gen}}) \times C_{\text{LLM}} + \mathcal{O}_{\text{NLI}}(S^2)$$

where \mathcal{O}_{NLI} represents the quadratic cost of comparing all sample pairs using an entailment model. This linear scaling with S introduces latency that is often unacceptable for interactive agents.

Scalar Probes (PCP, SEP). Scalar probes operate on prompt representations extracted from a single forward pass of the base model. The probe itself is a lightweight classifier or regressor applied to a cached hidden state, without requiring additional sampling or decoding:

$$\mathcal{O}_{\text{SEP}} \approx 1 \times T_{\text{pre}} \times C_{\text{LLM}} + C_{\text{MLP}}$$

While efficient, these methods predict a compressed scalar statistic and discard the geometric structure of the model’s semantic output distribution.

Semantic Self-Distillation (SSD). SSD matches the inference complexity of scalar probes while retaining the distributional richness of sampling methods. The MDN head introduces a slightly larger parameter set than a linear probe, but this cost (C_{MDN}) is negligible compared to the transformer backbone. Crucially, the entropy calculation is analytical and does not require sampling:

$$\mathcal{O}_{\text{SSD}} \approx 1 \times T_{\text{pre}} \times C_{\text{LLM}} + C_{\text{MDN}}$$

Thus, SSD effectively moves the computational burden from *inference time* (where latency matters) to *training time*, enabling $O(1)$ uncertainty estimation during deployment.

D ABLATIONS AND ARCHITECTURE ANALYSIS

D.1 PCA DIMENSION

Standard sentence embeddings are high-dimensional (e.g., $d_z = 768$). Training an MDN to model a full covariance density in this space is data-intensive. We apply PCA to reduce the target space to $d_{\text{pca}} \in \{16, 32, 64, 128\}$.

This introduces a trade-off: higher dimensions preserve more semantic detail (increasing the theoretical upper bound of detection performance, measured by teacher dispersion), but make the regression task significantly harder for the student. As shown in Figure 3 and Table 6, while the detection performance of teacher dispersion improves monotonically with dimensionality, the student’s performance (SSD) peaks at $d_{\text{pca}} = 16$. Beyond this point, the student fails to effectively distil the increasingly sparse density, leading to a drop in detection accuracy. For the OOD experiments we find PCA dimensions of 16 and 32 perform similarly, followed by a drop-off at higher dimensions. We fix $d_{\text{pca}} = 16$ for all main experiments bar the OOD task, where we set $d_{\text{pca}} = 32$.

We underline that the same training dataset size ($N_{\text{train}} = 4000$) was used in all PCA ablations; the learning task is therefore more difficult in higher dimensions, as models must learn more complex relationships using the same number of datapoints. For larger training datasets, we expect the SSD performance will continue to match or exceed the TD performance.

Table 6: Effect of PCA dimensionality on Hallucination Detection (SSD) and OOD Verification. Scores are averaged across the best student configuration for each model.

PCA Dim	Teacher Dispersion (TD)	Peak SSD AUROC	Peak OOD AUROC
16	0.699 ± 0.029	0.708 ± 0.026	0.965 ± 0.026
32	0.724 ± 0.027	0.706 ± 0.029	0.966 ± 0.035
64	0.747 ± 0.025	0.701 ± 0.037	0.960 ± 0.047
128	0.757 ± 0.025	0.703 ± 0.029	0.950 ± 0.055

D.2 STUDENT CAPACITY AND INFORMATION SATURATION

We investigate whether the performance gap on difficult models can be closed by increasing the student’s capacity. We analyze two axes of complexity:

1. **Distributional Complexity:** We vary the number of mixture components $K \in \{1, 2, 5, 10\}$.
2. **Backbone Capacity:** We vary the MLP hidden dimension $H \in \{128, 256, 512, 1024\}$ and depth $D \in \{2, 3, 4, 6\}$.

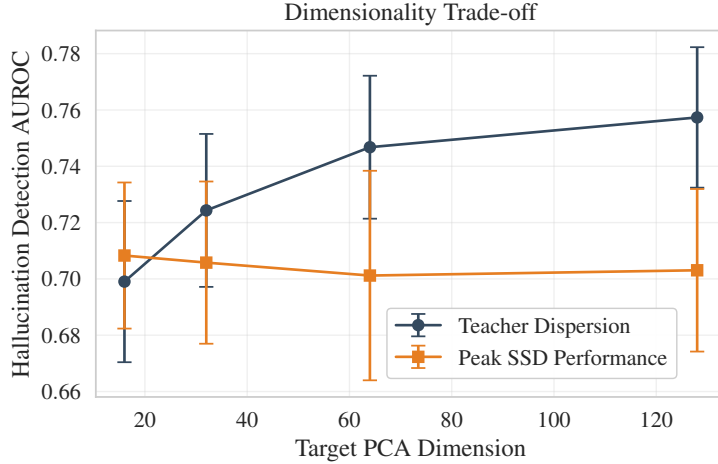


Figure 3: As PCA dimension increases, the semantic resolution improves and the teacher dispersion baseline rises. The distillation task however becomes harder, causing SSD performance to fall.

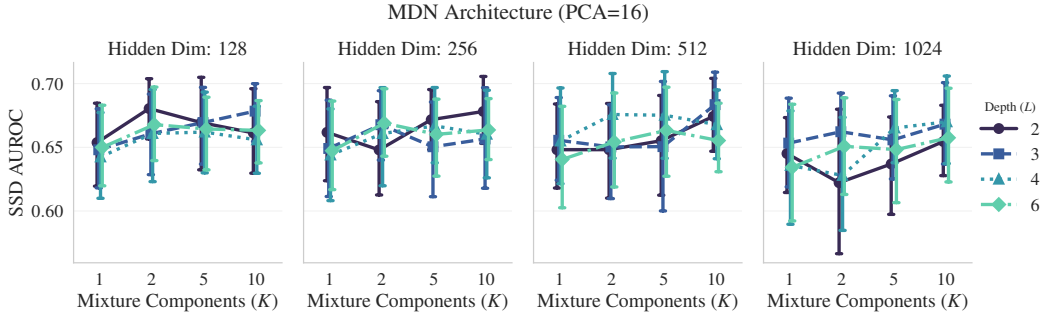


Figure 4: Student capacity ablation, averaged across all seven models investigated.

Table 5 reveals that the optimal hyperparameters vary by base model. Aggregating results across all models (Table 7) reveals **capacity saturation**, where increasing the network width or depth yields negligible gains in mean AUROC. This saturation suggests that the bottleneck is not the student’s expressivity, but the *mutual information* available in the final-token prompt representation. The student appears to have extracted most of the readily accessible signal; further improvements would require richer inputs (e.g., attention-pooled representations) rather than larger students. Although we observe optimal performance for $K = 10$ mixture components, we opt not to increase this further given our set number of $S = 32$ samples; modelling more than ten unique semantic concepts in this setting is unrealistic and would likely damage the generalization ability of the trained student.

Table 7: Marginal impact of student capacity (Fixed PCA=16). Scores represent the mean AUROC across all runs with the specified parameter; standard deviations indicate variability across different base models and remaining hyperparameter configurations. We observe negligible performance gains from increasing complexity, indicating information saturation in the prompt representation.

(a) Components (K)		(b) Width (H)		(c) Depth (D)	
K	AUROC	H	AUROC	L	AUROC
1	0.648 ± 0.050	128	0.662 ± 0.043	2	0.657 ± 0.049
2	0.657 ± 0.052	256	0.660 ± 0.046	3	0.660 ± 0.047
5	0.660 ± 0.048	512	0.660 ± 0.050	4	0.658 ± 0.050
10	0.666 ± 0.042	1024	0.649 ± 0.054	6	0.656 ± 0.048

E FULL HALLUCINATION DETECTION RESULTS

Table 8: **Hallucination Detection AUROC.** Values report mean AUROC (%) over 1,000 bootstrap resamples of the test set, with the bootstrap standard deviation shown as a subscript. We mark the best overall result in bold and the best single-pass result with an underline. SSD achieves competitive performance with teacher dispersion but lags scalar probes and SE.

Model	PCP	SEP	SSD (Ours)	TD	SE
Qwen3-8B	<u>76.9_{1.5}</u>	76.2 _{1.5}	67.7 _{1.8}	68.4 _{1.7}	81.6_{1.4}
Qwen3-4B	80.2_{1.4}	78.3 _{1.5}	69.9 _{1.6}	73.2 _{1.6}	78.5 _{1.5}
Llama 3.1 8B	<u>77.0_{1.6}</u>	74.5 _{1.7}	68.6 _{2.0}	69.5 _{1.7}	85.2_{1.3}
Llama 3.2 3B	<u>76.7_{1.5}</u>	75.7 _{1.5}	73.8 _{1.7}	66.5 _{1.7}	80.7_{1.4}
Minstral 8B	<u>74.0_{1.7}</u>	<u>77.1_{1.5}</u>	74.8 _{1.6}	74.3 _{1.6}	80.5_{1.5}
SmolLM3 3B	<u>79.7_{1.4}</u>	<u>78.9_{1.4}</u>	71.1 _{1.6}	69.8 _{1.6}	83.2_{1.2}
Gemma 3 4B	75.4_{1.5}	70.7 _{1.7}	70.1 _{1.7}	67.6 _{1.7}	73.1 _{1.6}

Table 9: **Hallucination Detection AUPRC.** Values report mean AUPRC (%) over 1,000 bootstrap resamples of the test set, with the bootstrap standard deviation shown as a subscript. We mark the best overall result in bold and the best single-pass result with an underline. SSD consistently outperforms the teacher dispersion (TD) baseline, effectively shifting the cost of dispersion estimation from inference time to training time.

Model	PCP	SEP	SSD (Ours)	TD	SE
Qwen3-8B	64.9 _{2.7}	<u>64.9_{2.7}</u>	57.0 _{2.8}	52.5 _{2.7}	75.0_{2.1}
Qwen3-4B	74.3_{2.3}	<u>70.8_{2.5}</u>	61.8 _{2.5}	59.6 _{2.5}	73.3 _{2.1}
Llama 3.1 8B	<u>59.6_{3.1}</u>	54.0 _{3.0}	51.9 _{3.0}	44.3 _{2.8}	73.5_{2.7}
Llama 3.2 3B	<u>68.9_{2.4}</u>	65.4 _{2.6}	65.7 _{2.7}	55.8 _{2.7}	74.2_{2.4}
Minstral 8B	59.2 _{2.9}	<u>62.9_{2.8}</u>	59.9 _{2.9}	57.9 _{2.9}	69.6_{2.7}
SmolLM3 3B	<u>75.1_{2.2}</u>	73.3 _{2.2}	62.3 _{2.6}	56.9 _{2.5}	78.9_{1.9}
Gemma 3 4B	69.4_{2.4}	65.0 _{2.5}	66.2 _{2.5}	63.2 _{2.4}	69.2 _{2.3}